View metadata, citation and similar papers at core.ac.uk

brought to you by CORE

provided by Birkbeck Institutional Research Online

BIROn - Birkbeck Institutional Research Online

Curran, N.M. and Nottingham, M. and Alexander, L. and Crawford, Ian and Füri, E. and Joy, K.H. (2019) A database of noble gases in lunar samples in preparation for mass spectrometry on the Moon. Planetary and Space Science 182 , p. 104823. ISSN 0032-0633.

Downloaded from: http://eprints.bbk.ac.uk/id/eprint/30695/

Usage Guidelines:
Please refer to usage guidelines at https://eprints.bbk.ac.uk/policies.html or alternatively contact lib-eprints@bbk.ac.uk.

A Database of Noble Gases in Lunar Samples in Preparation for Mass Spectrometry on the Moon

N. M. Curran[1,2], M. Nottingham[1,3,4], L. Alexander[3,4], I. A. Crawford[3,4], E. Füri[5], K. H. Joy[1]

[1]School of Earth and Environmental Sciences, University of Manchester, Oxford Road, Manchester, M13 9PL, UK

[2]NASA Goddard Space Flight Center, 8800 Greenbelt Road, Greenbelt, MD 20771, USA

[3]Department of Earth and Planetary Science, Birkbeck College, University of London, London, UK

[4]The Centre for Planetary Sciences at UCL-Birkbeck, London, UK

[5] Centre de Recherches Pétrographiques et Géochimiques, CNRS-UL, 15 rue Notre Dame des Pauvres, BP20, 54501 Vandoeuvre-lès-Nancy Cedex, France

Corresponding email: natalie.m.curran@nasa.gov

Keywords: lunar-regolith, noble-gases, lunar-mission, noble-gas-mass-spectrometer, lunar-rock, database

Abstract

The lunar regolith provides a temporal archive of the evolution of the Moon and inner Solar System over the last ~4 billion years. During this time, noble gases have been trapped and produced within soils and rocks at the lunar surface. These noble gas concentrations can be used to unravel the history of lunar material and shed light on processes that have evolved the surface of the Moon through time. We have collected published noble gas data for a range of lunar samples including soils, regolith breccias, crystalline (e.g., mare basalts, anorthosite) and impact-melt rocks. The compilation includes noble gas concentrations and isotope ratios for He, Ne, Ar, Kr and Xe; trapped, cosmogenic and radiogenic isotopes; and cosmic ray exposure ages. We summarise the significance of these data, which can be used as a baseline for expected noble gas concentrations in a range of lunar samples, and provide a framework for future *in situ* noble gas measurements on the lunar surface.

1. Introduction

The lunar regolith represents a unique archive of surface and planetary processes that have shaped the lunar crust through its history. The majority of our knowledge regarding the Moon comes from samples collected from the regolith by lunar missions (Apollo and Luna), remote sensing data of the regolith, and lunar meteorites launched from near-surface regolith environments (Papike et al. 1998; Korotev, 2005; Lucey et al. 2006). These samples contain records of volatiles that have been endogenically and exogenically added to the lunar surface (McKay et al. 1991; Anand et al. 2012; Füri et al. 2012; McCubbin et al. 2015). Such volatiles include the inert noble gases helium, neon, argon, krypton and xenon. Noble gases are added to the regolith by: the trapping of solar wind and lunar exosphere particles; the production of cosmogenic nuclides from solar and galactic cosmic rays (SCRs and GCRs, respectively) (e.g., Wieler, 1998, 2002a, 2002b; Swindle et al. 2002; Wieler and Heber, 2003; Eugster, 2003); the *in situ* decay of radioactive elements; and noble gases that may be indigenous to the Moon or delivered by asteroids and/or comets (Füri et al. 2012, 2018; Bekaert et al. 2017; Pernet-Fisher and Joy, 2018). A key aspect in understanding the evolution and budgets of noble gases, and other volatile elements such as H, C, N and O, is to determine the end-member source/s and to decipher when in time these volatiles were delivered to, or produced on, the Moon. The lunar regolith noble gas budget also aids our understanding of the impact modification of the Moon through time (McKay et al. 1986; Eugster et al. 2001; Joy et al. 2011; Fagan et al. 2014) and the changing galactic environment (Crawford et al. 2014). Furthermore, given that these volatiles could potentially provide valuable resources, understanding their abundance and distribution has important *in situ* resource utilisation implications (e.g. Fegley and Swindle, 1993; Crawford, 2015).

The Roscosmos Luna-27 south polar lander aims to investigate potential resources and volatile budgets at the lunar surface. The European Space Agency's (ESA's) contribution to Luna-27 is the PROSPECT (Platform for Resource Observation and in-Situ Prospecting in support of Exploration, Commercial exploitation and Transportation) instrument, which provides the capability to drill into the sub-surface of the Moon to approximately 1 m depth, and collect regolith samples (Carpenter et al. 2015; Carpenter and Fisackerly, 2017; Barber et al. 2017, 2018; Sefton-Nash et al. 2018). The regolith samples collected will be transferred to a miniature chemistry laboratory, known as ProSPA (PROSPECT Sample Processing and Analysis), that will be used to identify volatile species present (e.g., H, C, N, O, noble gases), and analyse their abundances and isotopic compositions (Barber et al. 2017, 2018). The ProSPA instrument will extract gases using a range of temperatures from approximately -230°C through to temperatures of ~1000°C (Barber et al. 2017, 2018).

In order to understand the noble gas budget currently available and to assess the noble gas analytical capability of ProSPA, the available natural (i.e., not neutron irradiated) noble gas data for lunar samples was collated into a database (Table S1-S4). The main purposes of this database are to:

a) Compile the current published noble gas datasets and uncertainties for lunar samples and make this compilation available to the noble gas and planetary science communities.
b) Evaluate these data to provide recommendations for experimental noble gas analysis on the forthcoming ProSPA experiment (Barber et al. 2017, 2018; Carpenter et al. 2017) and future *in situ* exploration.

2. Guide to lunar database

Noble gases incorporated into lunar materials have several potential origins. Three terms are classically used to describe the major noble gas reservoirs in lunar samples (although there are potentially additional components, e.g., indigenous, extralunar), which are 'trapped' (tr), 'radiogenic' (*), and 'cosmogenic' (c). These components relate to the origin and method of incorporation into a sample. The trapped and cosmogenic components are defined by 'end-member' compositions that need to be known in order to understand the reservoir mixing processes that have affected a given sample over its history.

To address both instrument and mission science drivers for noble gas analysis on ProSPA and future planetary missions, we have compiled a database (Table S1-S4) of existing noble gas literature data for lunar regolith (soils, regolith breccias and sub-surface), crystalline (basalts, anorthosite) and impact-melt samples. For lunar meteorite noble gas data, we refer to the compilation by Mészáros et al. 2018. The values in Table S2-S3 were originally obtained using various methods of extracting and analysing noble gases from lunar samples. Extraction methods include both bulk-extraction (chips and <1000 μm soil) and step heating of samples using a furnace-oven or laser system from both rock samples and mineral or grain size separates. The metadata provided includes (where available):

Sample specific information: this information includes sample name, subsplit, sample classification (e.g., crystalline, soil), sample type (e.g., mare basalt, glass), mass analysed (mg), and sample analysed (e.g., bulk chip/soil, grain size or mineral separates). Some studies provide temperature step-heating data for individual samples, these were also included in the database. Please note that etched sample, K-Ar, Ar-Ar or I-Xe data are not included in this database.

Noble gas data: isotope concentrations for He, Ne and Ar are given in 10^{-6} cm^3STP/g, with Kr and Xe concentrations given in 10^{-8} cm^3STP/g, and errors are reported where possible. Noble gas isotopic ratios are also recorded. For Kr and Xe ratios are often scaled by a factor of 100 in the original souce, resulting in a reference isotope of 100. Users should be aware that we have normalised all scaled data to a reference ratio of 1. This ensures direct comparability of all data contained within the database (please note, this was not considered a 'calculation' for the purposes of database formatting, and as such is not highlighted in red). Data recorded in red in the database are not directly reported in the original source. However, these data have been determined using a combination of other isotopes and/or ratios (users should note, some data have also been converted from different

units into our standardised cm^3STP/g form). Concentrations of cosmogenic isotopes $^{3}He_c$, $^{21}Ne_c$, and $^{38}Ar_c$ (in concentrations of 10^{-8} cm^3STP/g), and $^{78}Kr_c$, $^{80}Kr_c$, $^{81}Kr_c$, $^{124}Xe_c$ and $^{126}Xe_c$ (10^{-12} cm^3STP/g), radiogenic $^{40}Ar^*$ (10^{-8} cm^3STP/g) and trapped $^{36}Ar_{tr}$ (10^{-8} cm^3STP/g) are also compiled in the database (Table S2). Cosmic ray exposure ages for T^3He, $T^{21}Ne$, $T^{38}Ar$, $T^{78}Kr$, $T^{81}Kr$, $T^{124}Xe$ and $T^{126}Xe$ are reported in million years (My). For Apollo and Luna samples cosmic ray exposure ages are in Table S2, lunar meteorites can be found in Table S3. Errors reported in red for all data have been determined based on information in the original source. Some errors are calculated using a combination of ratios and concentrations in order to provide a more complete picture of the data. User discretion is advised when using these errors in analyses.

The values in Table S2-S3 have not undergone any data quality checks or filtering from the original reported data. The information in the Table S2-S3 includes data from over 1600 lunar samples (this includes several samples that have been analysed multiple times) from over 100 refereed published journals over the past ~50 years. The full reference list is provided in Table S4. Whilst every effort was made to ensure accuracy of the database, it may be that some data was missed or data was incorrectly transcribed into the database. We kindly ask users to report any errors and/or additional data you may find to the authors so that we can rectify the issue, and maintain the efficacy of the database.

2.1 Uncertainty on reported data

An unavoidable consideration when compiling data from multiple sources is the variation in uncertainty propagation methods and their effects on future use of the collated data. Most research laboratories establish their own methods of uncertainty propagation and data correction, and it is rare for these methods to be comprehensively published alongside the data (particularly in the case of older published papers). We have retained published uncertainties where available for congruity with the literature. It is often assumed that uncertainty is standardly reported to 1σ confidence levels, however, this assumption may lead to an unnecessary devaluing of published data that has actually been measured more precisely. Where possible, we have maintained the error propagation detailed within the original sources. There are however, situations where we have applied mathematical error propagation methods to gaps within the published data. This propagation has only been carried out where the published errors and data allow for unambiguous calculation of uncertainty. It should be noted that these calculations were carried out following a set protocol across the entire database and no bias was allowed for any data contained within the database. Users are advised that, where these calculations have been included, the formulae used are preserved within the database and we recommend users confirm their satisfaction with these calculations before using the uncertainties they relate to. It is likely that many of these propagated errors are greater than the actual analytical precision of the published data owing to the required inclusion of gas concentration data as well as gas ratio data.

2.2 Lunar samples

Many lunar sample types have been analysed for their noble gas concentrations over the last 50 years. These span a range of masses from <1 mg (soils and regolith breccias) to ~1000's of mg (crystalline samples). Most of these samples consist of four main minerals, which account for the majority (98-99%) of the crystalline material at the lunar surface: plagioclase, pyroxene, olivine and ilmenite (Papike et al. 1991; Lucey et al. 2006; Korotev, 2019). The other 1-2% is mostly made up of accessory minerals such as oxide minerals (chromite, troilite), K-feldspar, Ca-phosphates (apatite, merrillite), zircon-bearing phases (baddeleyite, zircon, and tranquillityite) and Fe-metal. The dominant mineral in the feldspathic lunar highlands is a Ca-rich plagioclase feldspar known as anorthite. These minerals contain the target elements (e.g., O, Si, Mg, Fe, Ca) to produce the various cosmogenic noble gases. The rock type and chemical make-up of samples is important to know for determining the cosmogenic isotope production rates and for understanding the cosmic ray exposure age of a sample. A summary of the dominant rock types found in the lunar noble gas database (Table S2) is provided in the Table S1.

3. Lunar science enabled from noble gases

Noble gases not only offer a way to understand the history of a sample during its lifetime at the lunar surface (e.g., Eberhardt et al. 1974; Hintenberger et al. 1975; Bogard et al. 1978; Eugster et al. 1986, 1988; Eugster, 2003; Lorenzetti et al. 2005), but also provide important information for deciphering a number of key questions regarding the history of the Moon, the wider Solar System, and the galactic environment (e.g., McKay et al. 1991; Hörz et al. 1991; Wieler, 1998, 2002a, 2002b, 2016; Lucey et al. 2006). Outlined here are some examples but for in depth review we refer readers to the list of reference in text and Table S4).

3.1 Regolith history and delivery of volatiles

The history recorded in lunar samples can be determined using a combination of noble gas isotopes (e.g., radiogenic, cosmogenic). Noble gases are especially useful for these studies because prior to exposure to the space environment they typically have low concentrations (except for potential indigenous and radiogenic isotopes produce *in situ*) in lunar samples. Noble gas data can help to decipher the history of an individual sample during its lifetime in the regolith by determining the following:

Cosmic ray exposure (CRE) age and shielding depth: Although the Moon may have had an early magnetic field (4.25 to ~3.3 Ga - e.g., Garrick-Bethell et al. 2009; Weiss and Tikoo, 2014), for most of its history it is thought to neither have a significant magnetic field, nor a sufficiently thick exosphere (lunar "atmosphere") to attenuate the effects of cosmic rays. As a result, cosmic rays generate their end-products in solid material exposed at the lunar surface (2π-irradiation) and, in the

case of lunar meteorites, during exposure when travelling through free space (4π-irradiation). The majority of lunar samples have experienced complex exposure histories, i.e., more than one period of 2π-irradiation at varying shielding depths (Hörz et al. 1991; Eugster, 2003). This is caused by the repeated burial, exhumation and overall transportation of individual soil grains both vertically and laterally in the lunar regolith during the 'gardening' process (Morris, 1978; Haskin and Warren, 1991; Hörz et al. 1991; McKay et al. 1991; Lucey et al. 2006). Therefore, probing the cosmic ray exposure age and shielding record of lunar samples provides further understanding of the processes that occur at the lunar surface (e.g., the regolith overturn rate and evolution). In some cases, the CRE age can reflect accurate upper limits for a samples antiquity (Wieler, 2016). For example, if samples collected at the rim of a crater all yield the same CRE age, this age likely dates the formation of the crater. The grains from these samples would have incorporated trapped gases since this exposure began. It should be noted that these values are affected by a number of assumptions made during the calculation. Most calculated CRE ages assume a single shielding depth (normally either 0 g/cm^2, or a depth informed by a system such as the ^{21}Ne/^{22}Ne shielding depth indicator). This assumption does not account for the varying of sample size (i.e. the breakup of larger boulders into smaller samples) or changes in the sample's burial depth over time. It is worth noting that many samples examined indicate an average shielding depth different to the depth from which they were collected (e.g. a sample may indicate an average shielding depth of 10's of cm below the surface, but may have been collected in a soil sample from the lunar surface). For this reason, it is sometimes more beneficial to view these ages as lower limits on the total exposure duration of a sample.

Maturity: Maturity is a qualitative measure of planetary surface exposure to the space environment. Prolonged exposure to solar wind irradiation and micrometeorite bombardment at the lunar surface (defined for this purpose as the top millimetre) results in the maturation of the soil. Several indicators have been shown to be proportional to surface maturity, including decreased grain size, abundance of agglutinates, concentrations of trapped noble gases and the I_s/FeO index. The most widely used maturity index during the Apollo era was the I_S/FeO value, which is the ratio of the ferromagnetic resonance intensity (because of the production of native nanophase Fe from the reduction of Fe^{2+} in silicates and oxides in lunar soils, Morris, 1976, 1978, 1980) normalised to the bulk rock FeO content.

Antiquity age: The antiquity age of regolith samples represents the time when a soil was lithified into a breccia and closed off from further weathering from the solar wind (McKay et al. 1986; Eugster et al. 2001; Joy et al. 2011; Fagan et al. 2014; Wieler, 2016). The most widely used antiquity indicator uses the trapped $(^{40}Ar/^{36}Ar)_{tr}$ ratio. Argon-40 is originally produced by the *in situ* radioactive decay of ^{40}K in the lunar interior. Some of this ^{40}Ar is degassed into the lunar exosphere. This ^{40}Ar is then ionised by solar UV rays and re-implanted into surface-exposed lunar regolith where it becomes 'trapped' on and within the grains (i.e., $^{40}Ar_{tr}$) (e.g., Manka and Michel, 1970, 1971). The trapped ^{40}Ar ($^{40}Ar_{tr}$) is normalised to the amount of solar wind derived ^{36}Ar ($^{36}Ar_{tr}$) in the sample, where $^{36}Ar_{tr}$ is

assumed to be implanted at a constant rate through lunar history. The flux of radiogenic ^{40}Ar ($^{40}Ar^*$) is expected to have decreased over time at around the same rate as ^{40}K decay within the lunar crust (McKay et al. 1986; Eugster et al. 2001; Joy et al. 2011) and so the $(^{40}Ar/^{36}Ar)_{tr}$ ratio has decreased through time, with ancient regolith breccias recording higher $(^{40}Ar/^{36}Ar)_{tr}$ ratios.

The antiquity age can provide information on when in time the solar wind particles and volatiles in the sample were collected, and used to constrain the timing of the delivery of these volatiles to the surface (Joy et al. 2011; Fagan et al. 2014). While there is some question to whether the decrease in the $(^{40}Ar/^{36}Ar)_{tr}$ ratio actually reflects the decay of ^{40}K (we refer readers to Wieler, 2016; Korochantseva et al. 2017), the $(^{40}Ar/^{36}Ar)_{tr}$ ratio remains a semi-quantitative indicator of regolith antiquity in addition to cosmic ray exposure ages.

The noble gas budget can be used to help decipher regolith evolution and crustal modification processes that occur on the Moon, as well as other planetary surfaces. This allows better understanding the rates at which asteroids, comets and cosmic dust have hit the Moon and sheds further light on the bombardment history of planetary bodies in the inner Solar System (McKay et al. 1991; Lucey et al. 2006; NRC, 2007; Fagan et al. 2014).

3.2 The history of the Sun

Unlike Earth, the Moon does not have a thick atmosphere to protect it from space weathering, although it may have during the peak of lunar mare volcanism (Needham and Kring, 2017). As a result, the lunar regolith acts as the boundary layer between the space environment and the solid body of the Moon (Lucey et al. 2006; Spray, 2016). Therefore, solar wind and solar cosmic rays interact directly with surface-exposed regolith. During the past ~4 billion years the regolith has been stirred, buried and exhumed ("gardened") to the point where it can be reasonably assumed that every grain within the lunar regolith has at some point, and for a variable duration of time, been exposed to the solar wind (Eberhardt et al. 1970; Pepin et al. 1970; Reynolds et al. 1970; Wieler, 1998). It is estimated that the top few centimetres of the regolith are overturned once per million years (Hörz et al. 1991), although with the production of secondary craters this could be increased to once per 81,000 years (Speyerer et al. 2016). This implies that, with gardening, implanted noble gases could have been trapped at the surface over various periods, and are now located at random depths in the lunar regolith (Walton et al. 1973; McKay et al. 1991; Wieler, 1998, 2002b; Lucey et al. 2006; NRC, 2007; Crawford et al. 2010; Crawford and Joy, 2014; Binns et al. 2016). Unravelling these temporal records is complicated because a single regolith soil sample may reflect a stochastic accumulation of surface exposure intensities. However, these accumulations represent our current best ability to approximate the surface solar wind exposure and by using these averages together with studying samples of various antiquity (see section 3.1), we can learn about the history and evolution of the Sun as recorded in the nature of solar wind particles and solar cosmic ray products locked in regolith samples (Crozaz, 1977; Crozaz et al. 1977; Reedy et al. 1983; McKay et al. 1991; Wieler, 1998; Crawford et al. 2010;

Fagents et al. 2010; Saxena et al. 2019). We note that variations in solar activity, that are potentially recorded in the lunar regolith, may have had significant implications for the origin and evolution of life on the early Earth (Airapetian et al. 2016)

3.3 The history of the Galaxy

In addition to providing information about the history of the Sun, noble gases have the potential to provide insight into the history of the Galaxy and its implications for the development of life on Earth. The Solar System has been subject to a wide range of galactic environments as it orbits the Galaxy, and the GCR flux is sensitive to a variety of astrophysical processes including the star formation rate and nearby supernova explosions (e.g., Scherer et al. 2006; Shaviv, 2006). As the Moon possesses some of the most ancient surfaces in the Solar System, it may preserve a record of enhanced galactic cosmic ray fluxes in cosmogenic noble gas isotopes, which could potentially provide information on the structure and evolution of the Galaxy (e.g. Wieler, 2002b; Crawford et al. 2010; Crawford and Joy, 2014). As for variations in solar activity discussed in section 3.2, varying GCR fluxes may also have influenced the development of life on Earth (Crawford et al. 2010, and references cited therein).

Noble gas data from various periods of lunar history can also be used to examine whether signatures of long exposure can be separated from a "spike" (representing an increased flux of GCRs, e.g., from when the Solar System passed close to a supernova explosions) in the rock record (e.g., Benítez et al. 2002; Cook et al. 2009; Fimiani et al. 2016; Wallner et al. 2016; Crawford, 2017, and references cited therein). Testing theories of the variation in the galactic cosmic ray flux in this way can help to develop criteria for selecting future samples, which can provide a detailed galactic record, provided they are extracted from different radiometrically dateable horizons such as palaeoregoliths (e.g. Crawford et al. 2010).

3.4 Lunar Resource implications

There is growing interest in the possibility that lunar resources may be useful in the context of future space exploration (see Crawford, 2015, for a review). Currently, most interest lies in finding deposits of water ice, and/or hydrated materials, at high lunar latitudes as these would be potential sources of H_2O, O_2 and H_2 with multiple applications for space exploration. Characterising these polar volatiles from a resource perspective is a major objective of the ProSPA experiment (Barber et al. 2017). However, volatiles implanted by the solar wind are also a potential resource, and in order to assess this potential Fegley and Swindle (1993) conducted a thorough review of the concentrations of solar wind-derived volatiles in the lunar regolith.

Whether the lunar noble gases will have resource potential is debatable. Argon (average concentration of ^{36}Ar in Apollo soils is ~300×10^{-6} cm^3 STP/g, Table S2) is used as an inert gas in a

range of industrial processes (e.g., arc welding), although none of these are likely to be implemented on the Moon in the near future. Inert gases are also widely used as propellant for ion thrusters. Xenon is preferred owing to its high mass, but its concentration in the lunar regolith is so low (average concentration of ^{132}Xe in Apollo soils is ~0.025 × 10^{-6} cm^3 STP/g from Table S2) that the Moon is unlikely to be a viable source of Xe for this application. Given the much greater abundance of Ar in the lunar regolith, it may be worth investigating if substituting Ar for Xe as a propellant could make the lunar regolith an economically viable resource for this application. Note, however, that at a ^{36}Ar concentration of 300 × 10^{-6} cm^3 STP/g, it would be necessary to process approximately 2,070 kg of regolith to yield 1 g of ^{36}Ar. However, the grain size of material used will also have an effect and investigating this factor is an important consideration for *in –situ* resource utilisation.

Historically, much interest has focussed on solar wind-implanted ^{3}He because of its potential use as a fuel for future nuclear fusion reactors (e.g. Wittenberg et al. 1986; Schmitt, 2006; Kim et al., 2019). The currently known concentrations of ^{3}He in the lunar regolith are so low (~4 ppb on average, but perhaps up to 20 ppb in high-Ti mare regoliths; e.g. Fa and Jin, 2007, see also Table S2), and the technical difficulties of implementing ^{3}He-based fusion so large, that economic exploitation of lunar ^{3}He is doubtful (see discussion by Crawford, 2015).

Nevertheless, in spite of the above caveats, we hope that Table S2 of lunar noble gases compiled here will be helpful in assessing the resource potential of solar wind-implanted volatiles, not least by collating information from analyses published since the review of Fegley and Swindle (1993).

4. Summary of lunar noble gas budgets and observations

4.1 Variations in noble gas abundances per unit mass of sample

Typical sample masses that may be analysed on current and future rover-based planetary missions are between <1 and 10 mg. As such, to get a better understanding of the diversity between sample types and noble gas abundances, in Figure 1 the available noble gas data are scaled to a 1 mg mass equivalent. These data show expectedly that there are significant variations in isotope concentrations across different lunar rock types. The present-day surface soils have the largest concentrations of all noble gases (e.g., average ^{4}He concentrations of ~70000 × 10^{-6} cm^3 STP/g), while lunar meteorites (Mészáros et al. 2018), crystalline rocks and impact-melts contain the lowest concentrations (e.g., minimum ^{4}He concentrations of ~0.02 × 10^{-6} cm^3 STP /g). Unsurprisingly, lunar meteorites have the largest variation in concentrations, likely because they are made up of a variety of different components (e.g., soils, breccias, impact melts, crystalline material). For example, lunar meteorites have ^{4}He concentrations that vary from ~0.06 × 10^{-6} cm^3 STP/g to ~1800 × 10^{-6} cm^3 STP/g (Figure 1a).

Grain size separates from soil, breccias and sub-surface samples (i.e., drill cores) also have a large variation in noble gas concentrations (Figure 2a-c). Some grain size fractions <200μm display

the largest concentrations of noble gases compared to the larger grain size fractions (Figure 2a-c). This is most pronounced in with Ne and Ar isotopes (Figure 2b and 6c).

4.2 Noble gases in lunar samples

Soils and regolith breccia records

Lunar soils and regolith breccias from the Apollo and Luna missions were all collected from the surface of the Moon and have therefore, at least in the last few million years, been exposed to surface processes, including exposure to cosmic rays and solar wind, as well as meteorite and micrometeorite bombardment (resulting in an increase in soil maturity).

For Ne and Ar, if there was no isotopic fractionation during the trapping process(es), and the sample was not affected by secondary thermal processes (resulting in the loss of the lighter isotopes), lunar rocks lie on a mixing line between the cosmogenic and solar wind end-members. A good illustration of such mixing lines is the neon three-isotope plot ($^{20}Ne/^{22}Ne$ versus $^{21}Ne/^{22}Ne$) (Figure 3a), and $^{20}Ne/^{22}Ne$ versus $^{38}Ar/^{36}Ar$ (Figure 3b). However, most experimental points for lunar soils and breccias lie just below the mixing line for neon isotopes (e.g., Figure 3a). This is the result of equilibrium between implantation and sputtering caused by solar wind irradiation. The majority of the lunar soils and regolith breccias plot close to the pure solar wind end-member (Figures 3a and 3b, and given in Table 1). Compared to crystalline rocks and meteorites, (fine-grained) regolith samples have a large surface/volume ratio, therefore, their noble gas content is dominated by the surface-sited solar component. Only three of the regolith breccias (15205, 15688, 68115) in Table S2 are more cosmogenic than the majority of the soils and breccias, indicated by the lower $^{20}Ne/^{22}Ne$ (<8) and higher $^{21}Ne/^{22}Ne$ (>0.3) ratios. Collectively, the Apollo soils show the closest $(^{20}Ne/^{22}Ne)_{tr}$ ratio (13.3) to that of pure solar wind ($^{20}Ne/^{22}Ne$ = 13.78, Table 1). Breccias have a slightly lower $(^{20}Ne/^{22}Ne)_{tr}$ ratio of 12.7 (Table 1). It is clear that both the soils and breccias have undergone some fractionation during trapping of solar wind noble gases as neither show a pure solar wind signature (plotting closer to fractionated solar wind, fSW: Figure 3a). Argon shows a similar trend to neon for soils and regolith breccias with $^{38}Ar/^{36}Ar$ ratios plotting close to solar wind (SW on Figure 3b). The $^{40}Ar/^{36}Ar$ ratios have a range from 0.09 to 6535 (Table 1), highlighting the range in both trapped and radiogenic ^{40}Ar concentrations in these samples (Figure 3c).

The Ca/Ti ratio has been used in lunar meteorites as an indicator of provenance, i.e., distinguishing between mare and highland rock types (e.g., Eugster, 2003; Eugster et al. 2006; Lorenzetti et al. 2005). Here, we compare it with the $(^{40}Ar/^{36}Ar)_{tr}$ (i.e., a proxy for the antiquity age) of different regolith samples (Figure 4). Several samples from Apollo 14, 15, 16 and 17 have antiquity ages that potentially lie between 2 and 3.5 Ga (although the error on these ages could be as high as 50%) but the majority of the lunar soils and breccias have an antiquity of less than 2 Ga regardless of

the geological terrain (Figure 4). Samples with the highest antiquity (>3.5 Ga) are from Apollo 14 and 16 as these have the highest $(^{40}Ar/^{36}Ar)_{tr}$ ratios. The dichotomy between the "ancient" (>3.5 Ga) and "young" (<2.5 Ga) samples of the Apollo 16 suite can clearly be identified (Figure 4, see also McKay et al. 1986, Fagan et al. 2014).

Of the available data for soils and regolith breccias, the exposure ages reported in the literature range from ~1 to 2300 My (810 My for breccias, Figure 5). However, the majority of lunar soils have an exposure age of <800 My (Figure 5). In view of this, because of their heterogeneous nature, it is often difficult to apply a correct (chemistry-dependant) production rate to calculate CRE ages for breccias and soils.

Sub-surface regolith samples

The sub-surface samples (drill cores, drive tubes and trench samples) act as a stratigraphic log of the lunar regolith at different sampling sites. The **drill core** samples (collected by the Apollo 15, 16, and 17 missions, and the **core** samples taken during the Luna 16, 20, and 24 missions) represent attempts to extract a continuous core of lunar regolith, from the surface down to a maximum depth of 3 m (in the case of the Apollo drill cores). ***Drive tubes*** sampled shallower depths (between 7 cm and 68 cm) on all of the Apollo missions. ***Trench samples*** were extracted from the upper ~50 cm of soil, although no stratigraphy was preserved in the collection process. These were collected to assess the differences between lunar surface and sub-surface samples (i.e. those not directly exposed to the solar wind flux at the time of collection).

Noble Gases with depth: Like the soils and regolith breccias, the Ne and Ar isotope ratios of the sub-surface samples are dominated by the solar component (Figure 3a and 3b), with a combined $^{20}Ne/^{22}Ne_{tr}$ ratio of 11.9. The concentrations of trapped gases are almost independent of depth. This implies very efficient stirring of the regolith. The analysis of ^{4}He, ^{20}Ne, ^{36}Ar, ^{84}Kr and ^{132}Xe provides a near ideal way of examining the trends with depth of trapped noble gases, as these isotopes are dominantly derived from the solar wind. Although, for ^{4}He it is important to note that this depends on the grain size of the particles, as large grains can be dominated by radiogenic helium. The variation of the trapped isotopes in the Apollo 15 and 16 bulk sub-surface samples (down to a depth of approximately 250 cm) are compared to Apollo 17 samples collected in the top 7 cm (Figure 6). For the most part, the Apollo 15 and 16 samples show a similar trend: the ^{4}He, ^{20}Ne and ^{36}Ar concentrations decrease down to ~50 cm, where the isotope concentrations begin to increase and reach peak concentrations at a depth of approximately 75 - 125 cm.

Noble gas isotope ratios within these sub-surface samples are, as expected, comparable in range to those of the Apollo soils and breccia sample collection (Figure 3a-c). Noble gas isotope ratios of sub-surface samples show only relatively small variations regardless of depth (Figure 3a-c). The $^{20}Ne/^{22}Ne$ and $^{38}Ar/^{36}Ar$ ratios show a relatively small range of 11.9-12.8 and 0.18-0.19 (Table 1), respectively for the sub-surface samples, and all plot around pure solar wind.

Lunar meteorites

Lunar meteorites, which are sourced from random localities across the lunar surface, provide information on the Moon on a global scale (i.e., including the lunar farside, Korotev, 2005; Joy and Arai, 2013). New lunar meteorites are continually being found, adding to the growing collection of lunar samples (The Meteorite Bulletin, 2019) and providing additional data on noble gases on the Moon (e.g., Mészáros et al. 2018).

Unlike the soils and regolith breccias, the available noble gas data (see Mészáros et al. 2018 for compilation of these data) for the lunar meteorites show a much larger range in isotopic ratios (Figure 3a-c). Meteorites have some of the highest $^{21}Ne/^{22}Ne$ ratios of all the lunar samples because they are dominated by the volume-correlated cosmogenic component (Figure 3a). In general, the meteorite samples have some of the longest exposure ages of all the available samples, although the older ages have some of the largest errors (Figure 5). The exposure ages range from a few million years to a few billion years, with the majority <1000 My (Figure 5, Table S3). As the transit time of lunar meteorites from the Moon to Earth is relatively short (<1 My, often 10s ky: Gladman et al. 1998; Lorenzetti et al. 2005; Korotev, 2005), most of this exposure occurs on the Moon.

Crystalline rocks and impact melt breccias

The crystalline and impact melts rocks in Table S2 include different types of mare basalt rocks (e.g., both high- and low-Ti mare basalt and high- and low-Al types) and highland rock types (norites, anorthosite). The crystalline rocks (basalts and anorthosite) show a broad range of both Ne ($^{20}Ne/^{22}Ne$, $^{21}Ne/^{22}Ne$) and Ar ($^{38}Ar/^{36}Ar$ and $^{40}Ar/^{36}Ar$) ratios (Figure 3a-c), similar to the range shown in lunar meteorites.

Impact-melt samples also show a range across samples in both $^{20}Ne/^{22}Ne$ and $^{38}Ar/^{36}Ar$ isotopic ratios (Figure 3a and 3b). However, these impact-melt breccias seem to fall into two distinct "groups" either located near the solar wind end-member or the cosmogenic end-member for both the $^{20}Ne/^{22}Ne$ and $^{38}Ar/^{36}Ar$ isotopic ratios. Although this could just be the limited number of samples recorded in Table S2 for impact melt samples.

The impact melt samples show the most limited range in CRE ages of all the lunar samples in Table S2 (Figure 5), with all ages less than 200 My. The crystalline samples range from around 1 to 795 My (Figure 5).

5. Application and value of the noble gas database for *in situ exploration*

There are several critical questions when deciphering the extent to which the extraction and analysis of all noble gases is feasible with ProSPA and future planetary missions, in order to produce meaningful results:

5.1 Understanding the sources of noble gases

It is important to identify the potential end-member noble gas contributors to the lunar regolith. For example, at the lunar poles, some regions are in permanent shadow and extremely cold (annual temperatures between 40 and 110 K in permanently shadowed regions or PSRs: Paige et al. 2010). These regions are believed to be the storage sites of polar ices and may also be key sink and sequestration sites (Hodges, 1980, 2002; Wacker and Anders, 1984) for endogenic lunar noble gases and exogenous (e.g., 'planetary') components from volatile-rich asteroids and/or comets (Füri et al. 2012; Barnes et al. 2016). Knowledge of the noble gas sources in the current suite of lunar rocks and regolith will help our understanding of any potential additional noble gas reservoirs (e.g., indigenous, cometary, and meteoritic) which may be encountered on the Luna-27 mission. The data in Table S2-S3 provides a reference framework for lunar noble gas concentrations.

5.2 Extraction of noble gases from lunar samples

One of the most important issues regarding the *in -situ* analysis of noble gases on planetary missions concerns the extraction temperatures used by on-board ovens. Robotic planetary missions traditionally have limitations on gas extraction methods that can reduce the amount of certain gases released from a sample. For example, oven systems on robotic landers/rovers can achieve a maximum temperature in the range of ~800 to 1000°C (e.g., Rosenbauer et al. 1999; Pullan et al. 2004; Farley et al. 2013; Vasconcelos et al. 2016). However, the full extraction of all volume-correlated noble gases generally occurs during complete melting of a sample at temperatures that exceed 1200°C. Given these limitations, it is important to understand what can be technically achieved by ProSPA to get the desired extraction for a scientifically meaningful result. Furthermore, determining the minimum temperature required for meaningful noble gas results is vital to deciphering the feasibility of noble gas extraction with instruments such as ProSPA. The following section summaries the noble gas release patterns in several rock types from Table S2 (note: this is a sub-set of samples from Table S2 and not the entire dataset).

Noble gas release up to 1000°C

During noble gas analyses of lunar samples in terrestrial laboratories, samples are loaded into the inlet system of a mass spectrometer, kept under vacuum, and are often initially heated up to temperatures of ~200°C to remove any adsorbed terrestrial noble gas contamination (from terrestrial "air"). Typically, the lowest starting temperature for extraction of noble gases of interest from regolith breccias, impact-melts and crystalline rocks is 200°C. Temperatures lower than these are generally not sufficient to release significant concentrations of noble gases (i.e., cosmogenic or radiogenic contributions) that are contained within the 'volume' of a rock or mineral grain. Any gas released during low temperature heating steps, usually represents less than 1% of the total gas released for each noble gas isotope. However, this is not the case for all soils. Some "soil-like" (i.e. not well

consolidated) regolith breccias or powered samples, start releasing gas (mainly helium and neon) at temperatures as low as 100°C (Figures 7a and 7b).

By 1000°C, potentially all of the helium (>95%) and up to 70% of the total neon can be extracted from a range of lunar samples (Figure 7a and 7b). The release of Ar isotopes by 1000°C can be as low as 5% but up to 95% for some lunar samples (Figure 7c). The same is true for Kr isotopes (Figure 7d), but the release of Xe is generally lower between 20% and 50% by 1000°C. There is the potential here to determine a helium cosmic ray exposure age from the sample. However, during impact events, helium (and neon) are more readily degassed from a sample than Ar, Kr and Xe, and exposure ages for helium can sometimes be underestimated as a result.

The subtle decrease of $^{20}Ne/^{22}Ne$ (Figure 8a) and increase of $^{38}Ar/^{36}Ar$ (Figure 8b) ratios indicate a release of cosmogenic components. At approximately 800°C, the $^{40}Ar/^{36}Ar$ ratio falls to its lowest value (Figure 8c), corresponding to the maximum release of ^{36}Ar and giving potentially the best indication of the $(^{40}Ar/^{36}Ar)_{tr}$ ratio within the sample. The $^{40}Ar/^{36}Ar$ ratios decrease until ~800°C where the trend then flattens out until 1200°C where the ratio begins to increase again (Figure 8c). Although there is the possibility that not all of the solar Ar has been released at this point, this may be a good estimation of the bulk rock $(^{40}Ar/^{36}Ar)_{tr}$ ratio, which could provide a semi-quantitative indicator of antiquity (although note the caveats discussed in section 3.1).

Noble gas release above 1000°C

By 1200°C, nearly 99% of all noble gases have been released from most rock types, which includes both surface-correlated (e.g., trapped) and volume-correlated components (e.g., cosmogenic) (Figure 7). Most laboratory noble gas experiments on lunar soils and regolith breccias exceed temperatures of 1400°C to ensure the complete release of the entire suite of noble gases by complete melting of the sample. Heating samples to this temperature, therefore, provides a valuable noble gas inventory. If the sample mass and chemistry can be estimated or measured, the noble gas inventory can be used to determine the history of the sample in the regolith (e.g., CRE age, shielding depth - as outlined in section 3.1)

5.3 Recommendations and challenges for ProSPA and future lunar mission mass spectrometers

Knowledge of sample type and mass: It is of vital importance to know the type (e.g., chemical composition and petrology) and the mass (and grain size) of the sample to be analysed. This information is not just important for noble gas analysis. Sample chemistry is needed to determine the CRE age of a sample (see section 3.1), but this information also provides the geological context to fully understand a sample and the local environment. Furthermore, the abundance of different noble gas species in different lunar rock types (e.g., impact-melt, regolith or basalt) varies by several orders of magnitude (Figure 1). This is a difference to take into consideration for future planetary missions.

Concerning the Luna-27 PROSPECT mission, the contrast between the different noble gas isotope abundances (Figure 1) pushes the ProSPA mass spectrometer to technical limits. Helium, Ne and Ar isotopes have the ability to saturate instrument detectors or leave high system blanks after analysis (depending on vacuum capabilities), especially with a 'larger' 10 mg sample. In contrast, Kr and Xe isotope concentration could potentially fall below detection limits (i.e., blank levels) for ProSPA (currently around 10^{-13} cm^3). This is not a major concern in terrestrial laboratories, as noble gas analyses are made using a combination of detectors (e.g., Faraday cups and electron multipliers) allowing the dynamic range to be as high as 10^6. Furthermore, volume-calibrated purification lines allow for volume-dilution, which can reduce the amount of gas introduced into a mass spectrometer.

The data summarised here provides a baseline and a potential sample mass limitation for a range of regolith materials that can be investigated using the ProSPA instrument. The results imply that it is important to investigate the potential landing sites (e.g., Djachkova et al. 2017) and their local geology in order to have an understanding of the rock types and potential noble gas concentration ranges that may be expected.

Oven temperature: To completely understand the noble gas inventory of the sample analysed by ProSPA, the desirable target oven temperature would be ≥1200°C. This allows for all the noble gas species and components to be extracted. In the case of a lower maximum temperature for the ProSPA ovens, and given the data collated in the lunar regolith database, the minimum temperature requirement to achieve scientifically valuable noble gas data from regolith samples is between 800°C and 1000°C, which is achievable with ProSPA. Although not all of the noble gases are released at this temperature, there is potentially enough data to provide a scientifically meaningful $(^{40}Ar/^{36}Ar)_{tr}$ ratio (as most of the trapped solar wind noble gases are released by this point, Figure 8c), and He and Ne CRE age. These data can then provide temporal constraints on the delivery of volatiles to the surface of the Moon in the polar region. As ProSPA will analyse samples on the Moon, terrestrial contamination is not expected. However, in order to provide CRE ages and other antiquity indicators for all rock types, temperatures in excess of 1000°C are desirable.

Behaviour of noble gases in permanently shadowed regions: The behaviour of noble gases trapped in lunar polar ice reservoirs is currently poorly understood. Due to the extremely cold temperature (approximately -233°C) at the polar regions, water ice has the potential to trap lunar exosphere noble gases as well as other volatiles (Laufer et al. 1987; Bar-Nun, 1988). More investigations are needed to understand at what temperature different components (e.g., meteoritic, cometary) of noble gases are liberated from these polar regolith samples and, in the case of limited oven temperatures, what scientific information can be gained from the sample if not all the noble gases have been released.

6. Summary

We have collected noble gas data from published literature to form a database. The database contains details of noble gases in a range of lunar rock samples with a diverse set of antiquity ages, exposure ages, and maturities. The data from these samples provide a "snapshot" in time through various periods of lunar history which can be used to further understand the history and evolution of the regolith and lunar surface in general. The database is intended to be a resource for the lunar and planetary science communities, and provides scientists with a summary of the currently available noble gas datasets. Furthermore, the database provides a framework for understanding the behaviour and budget of noble gases for future lunar exploration.

The interpretation of the noble gas signature of the lunar regolith can be complicated given that many samples experienced multi-stage exposure histories at the (sub-) surface. However, a combination of noble gas isotopes can help unravel the history of a sample to understand the source/s of noble gases components – providing all of the noble gases are extracted. It is apparent from the summarised noble gas data, that the lunar regolith is stratigraphically heterogeneous in terms of noble gas contents, both laterally (soils and breccias) and vertically (sub-surface samples). This is perhaps not surprising as regolith exhumation and burial is caused primarily by impacts on the lunar surface, the occurrence of which is statistically random across the entire Moon. This means that nearly all of the samples have been exposed to the solar wind, cosmic rays or both during some period in lunar history. This makes them perfect specimens for probing lunar surface processes. The noble gas record of lunar rocks provides us with a vital tool for understanding the delivery of volatiles to the lunar surface, and, in most cases, provides the temporal constraints for regolith samples (e.g., CRE age, antiquity indicator $(^{40}Ar/^{46}Ar)_{tr}$ ratio) when analysed *in -situ* on the Moon.

7. Acknowledgements

We thank the very helpful suggestions of Prof. Rainer Wieler, an anonymous reviewer, and the Editoral support of Angelo Pio Rossi which helped to improve this manuscript. This project was jointly funded by an STFC studentship and a NASA Postdoctoral Fellowship to Natalie Curran; an ESA contract; a Royal Society University Research Fellowship UF140190, STFC grant ST/M001253/1 and RPG-2019-222 to Katherine Joy; and Leverhume Trust grant RPG-2015-020 to Ian Crawford. Part of this work appeared in ESA technical note (ESA-HRE-PROSPECT-TN-0001 13/4/2017).

8. References

Airapetian, V., Glocer, A., Gronoff, G., Hébrard, E., Danchi, W., 2016. Prebiotic chemistry and atmospheric warming of early Earth by an active young Sun. Nature Geoscience. 9, 452-455.

Anand, M., Crawford, I.A., Balat-Pichelin, M., Abanades, S., Van Westrenen, W., Péraudeau, G., Jaumann, R., Seboldt, W., 2012. A brief review of chemical and mineralogical resources on the Moon and likely initial In Situ Resource Utilization (ISRU) applications. Planet. Space. Sci. 74, 42-48.

Bar-Nun, A., Dror, J., Kochavi, E., Laufer, D., 1987. Amorphous water ice and its ability to trap gases. Physical Review B. 35, 2427-2435.

Barber, S., Smith, P., Wright, I., Abernethy, F., Anand, M., Dewar, K., Hodges, M., Landsberg, P., Leese, M., Morgan, G., 2017. ProSPA: the Science Laboratory for the Processing and Analysis of Lunar Polar Volatiles within PROSPECT. 48th Lunar and Planetary Science Conference. Abstract 2171.

Barber, S.J., Wright, I.P., Abernethy, F., Anand, M., Dewar, K.R., Hodges, M., Landsberg, P., Leese, M.R., Morgan, G.H. and Morse, A.D., 2018. ProSPA: Analysis of Lunar Polar Volatiles and ISRU Demonstration on the Moon. 49th Lunar and Planetary Science Conference. Abstract 2083.

Barnes, J.J., Tartese, R., Anand, M., Mccubbin, F.M., Neal, C.R., Franchi, I.A., 2016. Early degassing of lunar urKREEP by crust-breaching impact (s). Earth and Planetary Science Letters. 447, 84-94.

Bekaert, D.V., Avice, G., Marty, B., Henderson, B., Gudipati, M.S., 2017. Stepwise heating of lunar anorthosites 60025, 60215, 65315 possibly reveals an indigenous noble gas component on the Moon. Geochimica et Cosmochimica Acta. 218, 114-131.

Benítez, N., Maiz-Apellaniz, J., Canelles, M., 2002. Evidence for nearby supernova explosions. Physical Review Letters. 88, 081-101.

Bernatowicz, T., Hohenberg, C., Morgan, C., Podosek, F., Drozd, R., Lugmair, G., 1977. The regolith history of 14307. 8th Lunar and Planetary Science Conference Proceedings. pp. 2763-2783.

Binns, W., Israel, M., Christian, E., Cummings, A., de Nolfo, G., Lave, K., Leske, R., Mewaldt, R., Stone, E., von Rosenvinge, T., 2016. Observation of the 60Fe nucleosynthesis-clock isotope in galactic cosmic rays. Science. 352, 677-680.

Bogard, D. D., Hirsch, W.C., 1978. Noble gases in Luna 24 core soils. In Mare Crisium: The View from Luna 24: 105-116.

Bogard, D. D., Nyquist. L. E., 1973. 40Ar/36Ar variations in Apollo 15 and 16 regolith. Lunar and Planetary Science Conference Proceedings: Vol. 4.

Bogard, D. D., Nyquist, L. E., Hirsch W. C., 1974. Noble gases in Apollo 17 fines-Mass fractionation effects in trapped Xe and KR. Lunar and Planetary Science Conference Proceedings: Vol. 5.

Carpenter, J., Fisackerly, R., Aziz, S., Houdou, B., 2015. Exploring Cold Trapped Volatiles from Stationary Landers and Mobile Rovers: ESA Activities for Resource Prospecting at the Poles, Annual Meeting of the Lunar Exploration Analysis Group. abstract 2027.

Carpenter, J. and Fisackerly, R., 2017, March. PROSPECT: ESA's Package for Resource Observation and In-Situ Prospecting for Exploration, Commercial Exploitation, and Transportation. 48th Lunar and Planetary Science Conference. Abstract 1964.

Cook, D., Berger, E., Faestermann, T., Herzog, G., Knie, K., Korschinek, G., Poutivtsev, M., Rugel, G., Serefiddin, F., 2009. ^{60}Fe, ^{10}Be, AND ^{26}Al in lunar cores 12025/8 AND 60006/7: search for a nearby supernova. 40th Lunar and Planetary Science Conference. Abstract 1129.

Crawford, I.A., 2015. Lunar Resources: A Review. Progress in Physical Geography. 39, 137-167.

Crawford, I.A., 2017. The Moon as a Recorder of Nearby Supernovae. In: Alsabti A., Murdin P. (eds) Handbook of Supernovae, Springer. arXiv preprint arXiv:1608.03926.

Crawford, I.A., Fagents, S.A., Joy, K.H., Rumpf, M.E., 2010. Lunar Palaeoregolith Deposits as Recorders of the Galactic Environment of the Solar System and Implications for Astrobiology. Earth Moon Planets. 107, 75-85.

Crawford, I.A., Joy, K.H., 2014. Lunar exploration: opening a window into the history and evolution of the inner Solar System. Phil. Trans. R. Soc. A. 372, 20130315.

Crozaz, G., 1977. The irradiation history of the lunar soil. Physics and Chemistry of Earth. 10, 197-214.

Crozaz, G., Poupeau, G., Walker, R., Zinner, E., Morrison, D., 1977. The record of solar and galactic radiations in the ancient lunar regolith and their implications for the early history of the Sun and Moon. Phil. Trans. R. Soc. Lond. A 285, 587-592.

Djachkova, M.V., Litvak, M.L., Mitrofanov, I.G. and Sanin, A.B., 2017. Selection of Luna-25 landing sites in the South Polar Region of the Moon. Solar System Research. 51(3), 185-195.

Eberhardt, P., Geiss, J., Graf, H., Grögler, N., Krähenbühl, U., Schwaller, H., Schwarzmüller, J., Stettler, A., 1970. Trapped solar wind noble gases, exposure age and K/Ar-age in Apollo 11 lunar fine material. Geochimica et Cosmochimica Acta Supplement. 1, 1037.

Eugster, O., 2003. Cosmic-ray exposure ages of meteorites and lunar rocks and their significance. Chemie der Erde-Geochemistry. 63, 3-30.

Eugster, O., Herzog, G., Marti, K., Caffee, M., 2006. Irradiation records, cosmic-ray exposure ages, and transfer times of meteorites. In Lauretta, D.S. and McSween, H.Y. eds., 2006. Meteorites and the early solar system II. University of Arizona Press. 829-851.

Eugster, O., Geiss, J., Krähenbühl, U. and Niedermann, S., 1986. Noble gas isotopic composition, cosmic ray exposure history, and terrestrial age of the meteorite Allan Hills A81005 from the Moon. Earth and planetary science letters: 78, 139-147.

Eugster, O., Niedermann, S., 1988. Noble gases in lunar meteorites Yamato-82192 and-82193 and history of the meteorites from the moon. Earth and planetary science letters: 89, 15-27.

Eugster, O., Terribilini, D., Polnau, E., Kramers, J., 2001. The antiquity indicator argon-40/argon-36 for lunar surface samples calibrated by uranium-235-xenon-136 dating. Meteoritics and Planetary Science 36. 1097-1115.

Fa, W., Jin, Y.-Q., 2007. Quantitative estimation of helium-3 spatial distribution in the lunar regolith layer. Icarus. 190, 15-23.

Fagan, A.L., Joy, K.H., Bogard, D.D., Kring, D.A., 2014. Ages of globally distributed lunar paleoregoliths and soils from 3.9 Ga to the present. Earth, Moon, and Planets. 112, 59-71.

Fagents, S.A., Rumpf, M.E., Crawford, I.A., Joy, K.H., 2010. Preservation potential of implanted solar wind volatiles in lunar paleoregolith deposits buried by lava flows. Icarus. 207, 595-604.

Farley, K., Hurowitz, J., Asimow, P.D., Jacobson, N., Cartwright, J., 2013. A double-spike method for K–Ar measurement: A technique for high precision in situ dating on Mars and other planetary surfaces. Geochimica et Cosmochimica Acta. 110, 1-12.

Fegley B., Swindle, T.D. 1993. Lunar volatiles: implications for lunar resource utilization. In: Lewis J, Matthews MS and Guerrieri ML (eds). Resources of Near Earth Space. Tucson: Tucson University Press, 367-426.

Fimiani, L., Cook, D.L., Faestermann, T., Gómez-Guzmán, J.M., Hain, K., Herzog, G., Knie, K., Korschinek, G., Ludwig, P., Park, J. and Reedy, R.C., 2016. Interstellar 60Fe on the surface of the Moon. Phys. Rev. Lett. 116:151104.

Frick, U., Becker, R.H., Pepin, R.O., 1988. Solar wind record in the lunar regolith-Nitrogen and noble gases. In Lunar and Planetary Science Conference Proceedings : vol 18, 87-120.

Füri, E., Marty, B., Assonov, S.S., 2012. Constraints on the flux of meteoritic and cometary water on the Moon from volatile element (N–Ar) analyses of single lunar soil grains, Luna 24 core. Icarus. 218, 220-229.

Füri, E., Zimmermann, L. and Saal, A.E., 2018. Apollo 15 green glass He-Ne-Ar signatures–In search for indigenous lunar noble gases. Geochemical Perspectives Letters. 8, 1-5.

Garrick-Bethell, I., Weiss, B.P., Shuster, D.L. and Buz, J., 2009. Early lunar magnetism. Science. 323, 356-359.

Haskin, L., Warren, P., 1991. Lunar Chemistry. In Heiken, G.H., Vaniman, D.T., French B.M., Lunar Sourcebook. Cambridge Univ. Press, Cambridge, U.K. 357-474.

Heber, V.S., Wieler, R., Baur, H., Olinger, C., Friedmann, T.A., Burnett, D.S., 2009. Noble gas composition of the solar wind as collected by the Genesis mission. Geochimica et Cosmochimica Acta. 73, 7414-7432.

Hintenberger, H., Schultz. L., Weber H. W., 1975. A comparison of noble gases in lunar fines and soil breccias-Implications for the origin of soil breccias. Lunar and Planetary Science Conference Proceedings: Vol 6.

Hodges Jr, R.R., 1980. Lunar cold traps and their influence on argon-40. 11th Lunar and Planetary Science Conference Proceedings. 2463-2477.

Hodges, R.R., 2002. Ice in the lunar polar regions revisited. Journal of Geophysical Research: Planets. 107. E5011.

Hohenberg, C.M., Davis, P.K., Kaiser, W.A., Lewis, R.S., Reynolds, J.H., 1970. Trapped and cosmogenic rare gases from stepwise heating of Apollo 11 samples. Geochimica et Cosmochimica Acta Supplement: 1, 283.

Hörz, F., Grieve, R., Heiken, G., Spudis, P., Binder, A., 1991. Lunar surface processes. In Heiken, G.H., Vaniman, D.T., French B.M., Lunar Sourcebook. Cambridge Univ. Press, Cambridge, U.K. 61-120.

Hübner, W., Heymann, D., Kirsten, T., 1973. Inert gas stratigraphy of Apollo 15 drill core sections 15001 and 15003. Lunar and Planetary Science Conference Proceedings: Vol. 4, 2021.

Jordan, J.L., Heymann, D., 1975. Inert gases in fines at three levels of the trench at Van Serg Crater. Lunar and Planetary Science Conference Proceedings: Vol. 6, 2201-2218.

Joy, K.H., Arai, T., 2013. Lunar meteorites: new insights into the geological history of the Moon. Astron. Geophys. 54, 28-32.

Joy, K.H., Kring, D.A., Bogard, D.D., McKay, D.S., Zolensky, M.E., 2011. Re-examination of the formation ages of the Apollo 16 regolith breccias. Geochimica et Cosmochimica Acta. 75, 7208-7225.

Kaiser, W.A., 1972. Rare gas studies in Luna-16-G-7 fines by stepwise heating technique. A low fission solar wind Xe. Earth and Planetary Science Letters. 13, 387-399.

Kim, K.J., Wöhler, C., Berezhnoy, A.A., Bhatt, M., Grumpe, A., 2019. Prospective 3He-rich landing sites on the Moon. Planetary and Space Science: 104686.

Korochantseva, E., Buikin, A., Trieloff, M., 2017. Trapped extraterrestrial argon in meteorites. Geochemistry International. 55, 971-976.

Korotev, R.L., 2005. Lunar geochemistry as told by lunar meteorites. Chemie der Erde-Geochemistry. 65, 297-346.

Korotev, R.L., 2019. Meteorites. [URL: http://meteorites.wustl.edu/lunar/howdoweknow.htm, Accessed on 01/10/2019]

Laufer, D., Kochavi, E., Bar-Nun, A., 1987. Structure and dynamics of amorphous water ice. Physical Review B. 36, 9219.

Lorenzetti, S., Busemann, H., Eugster, O., 2005. Regolith history of lunar meteorites. Meteoritics and Planetary Science. 40, 315-327.

Lucey, P., Korotev, R.L., Gillis, J.J., Taylor, L.A., Lawrence, D., Campbell, B.A., Elphic, R., Feldman, B., Hood, L.L., Hunten, D., 2006. Understanding the lunar surface and space-moon interactions. In Jolliff, B.L., Wieczorek, M.A., Shearer, C.K. and Neal, C.R., 2018. New views of the Moon. 60, 83-219.

Mahajan, R.R., 2015. Lunar meteorite Yamato-983885: Noble gases, nitrogen and cosmic ray exposure history. Planet. Space Sci. 117, 24-34.

Manka, R.H., Michel, F.C., 1970. Lunar atmosphere as a source of argon-40 and other lunar surface elements. Science: 169(3942), 278-280.

Manka, R. H., Michel, F. C., 1971. Lunar atmosphere as a source of lunar surface elements. Lunar and Planetary Science Conference Proceedings: Vol. 2, 1717.

McCubbin, F.M., Vander Kaaden, K.E., Tartèse, R., Klima, R.L., Liu, Y., Mortimer, J., Barnes, J.J., Shearer, C.K., Treiman, A.H., Lawrence, D.J., 2015. Magmatic volatiles (H, C, N, F, S, Cl) in the lunar mantle, crust, and regolith: Abundances, distributions, processes, and reservoirs. American Mineralogist. 100, 1668-1707.

McKay, D., Bogard, D., Morris, R., Korotev, R., Johnson, P., Wentworth, S., 1986. Apollo 16 regolith breccias: Characterization and evidence for early formation in the mega-regolith. Journal of Geophysical Research: Solid Earth. 91, 277-303.

McKay, D.S., Heiken, G., Basu, A., Blanford, G., Simon, S., Reedy, R., French, B.M., Papike, J., 1991. The lunar regolith. In Heiken, G.H., Vaniman, D.T., French B.M., Lunar Sourcebook. Cambridge Univ. Press, Cambridge, U.K. 285-356.

Meteorite bullitin., 2019. [URL: https://www.lpi.usra.edu/meteor/. Accessed on 01/01/2019].

Mészáros, M., Hofmann, B.A., Leya, I., 2018. A noble gas data collection of lunar meteorites. Meteoritics and Planetary Science. 53, 1104-1107.

Morris, R., 1976. Surface exposure indices of lunar soils-A comparative FMR study. Lunar and Planetary Science Conference Proceedings. 315-335.

Morris, R., 1978. The surface exposure/maturity/of lunar soils-Some concepts and Is/FeO compilation. Lunar and Planetary Science Conference Proceedings. 2287-2297.

Morris, R., 1980. Origins and size distribution of metallic iron particles in the lunar regolith. 11th Lunar and Planetary Science Conference Proceedings. 1697-1712.

Mortimer, J., Verchovsky, A., Anand, M., Gilmour, I., Pillinger, C., 2015. Simultaneous analysis of abundance and isotopic composition of nitrogen, carbon, and noble gases in lunar basalts: Insights into interior and surface processes on the Moon. Icarus. 255, 3-17.

Needham, D.H. and Kring, D.A., 2017. Lunar volcanism produced a transient atmosphere around the ancient Moon. Earth and Planetary Science Letters. 478, 175-178.

NRC, 2007. The scientific context for the exploration of the Moon. National Research Council, Washington 140.

Paige, D.A., Foote, M.C., Greenhagen, B.T., Schofield, J.T., Calcutt, S., Vasavada, A.R., Preston, D.J., Taylor, F.W., Allen, C.C., Snook, K.J. and Jakosky, B.M., 2010. The lunar reconnaissance orbiter diviner lunar radiometer experiment. Space Science Reviews. 150(1-4),125-160.

Papike, J.J., Ryder, G., Shearer, C.K., 1998. Lunar samples. Reviews in Mineralogy and Geochemistry. 36, 5.1-5.234.

Papike, J., Taylor, L. and Simon, S., 1991. Lunar minerals. In Heiken, G.H., Vaniman, D.T., French B.M., Lunar Sourcebook. Cambridge Univ. Press, Cambridge, U.K. 121-182.

Pepin, R., Nyquist, L., Phinney, D., Black, D., 1970. Rare gases in Apollo 11 lunar material. Geochimica et Cosmochimica Acta Supplement 1. 1435.

Pernet-Fisher J. F., Joy, K. H., 2018. Noble-Gas Isotope Systematics of Lunar Anorthosites: Hunting For Indigenous Signatures. 49th Lunar and Planetary Science Conference. Abstract 1951.

Pullan, D., Sims, M., Wright, I., Pillinger, C., Trautner, R., 2004. Beagle 2: the exobiological lander of Mars express, Mars Express: The Scientific Payload. 165-204.

Reedy, R.C., Arnold, J.R., Lal, D., 1983. Cosmic-ray record in solar system matter. Science. 219, 127-135.

Reynolds, J., Hohenberg, C., Lewis, R., Davis, P., Kaiser, W., 1970. Isotopic analysis of rare gases from stepwise heating of lunar fines and rocks. Science. 167, 545-548.

Rosenbauer, H., Fuselier, S., Ghielmetti, A., Greenberg, J., Goesmann, F., Ulamec, S., Israel, G., Livi, S., MacDermott, J., Matsuo, T., 1999. The COSAC experiment on the lander of the ROSETTA mission. Advances in Space Research. 23, 333-340.

Saxena, P., Killen, R.M., Airapetian, V., Petro, N.E., Curran, N.M. and Mandell, A.M., 2019. Was the Sun a Slow Rotator? Sodium and Potassium Constraints from the Lunar Regolith. The Astrophysical Journal Letters: 876(1), L16.

Scherer, K., Fichtner, H., Borrmann, T., Beer, J., Desorgher, L., Flükiger, E., Fahr, H.-J., Ferreira, S., Langner, U., Potgieter, M., 2006. Interstellar-terrestrial relations: variable cosmic environments, the dynamic heliosphere, and their imprints on terrestrial archives and climate. Space Science Reviews. 127, 327-465.

Schmitt, H.H., 2006. *Return to the Moon*. New York: Copernicus Books.

Sefton-Nash, E., Carpenter, J.D., Fisackerly, R., Trautner, R. and Team, E.L.E., 2018, March. PROSPECT: ESA's Package for Resource Observation and In-Situ Prospecting for Exploration, Commercial Exploitation, and Transportation. 49th Lunar and Planetary Science Conference. Abstract 2083

Shaviv, N.J., 2006. Long-term variations in the galactic environment of the Sun, Solar journey: The significance of our galactic environment for the heliosphere and earth. Springer. 99-131.

Speyerer, E.J., Povilaitis, R.Z., Robinson, M.S., Thomas, P.C. and Wagner, R.V., 2016. Quantifying crater production and regolith overturn on the Moon with temporal imaging. Nature. 538(7624), 215-218.

Spray, J.G., 2016. Lithification mechanisms for planetary regoliths: The glue that binds. Annual Review of Earth and Planetary Sciences. 44, 139-174.

Swindle, T.D., 2002. Noble gases in the Moon and meteorites: Radiogenic components and early volatile chronologies. In Reviews in mineralogy and geochemistry. 47, 101-124.

Vasconcelos, P., Farley, K., Malespin, C., Mahaffy, P., Ming, D., McLennan, S., Hurowitz, J., Rice, M.S., 2016. Discordant K-Ar and young exposure dates for the Windjana sandstone, Kimberley, Gale Crater, Mars. Journal of Geophysical Research: Planets. 121, 2176-2192.

Wacker, J.F., Anders, E., 1984. Trapping of xenon in ice: implications for the origin of the Earth's noble gases. Geochimica et Cosmochimica Acta. 48, 2373-2380.

Wallner, A., Feige, J., Kinoshita, N., Paul, M., Fifield, L., Golser, R., Honda, M., Linnemann, U., Matsuzaki, H., Merchel, S., 2016. Recent near-Earth supernovae probed by global deposition of interstellar radioactive 60 Fe. Nature. 532, 69.

Walton, J., Lakatos, S., Heymann, D., 1973. Distribution of inert gases in fines from the Cayley-Descartes region. 4th Lunar and Planetary Science Conference Proceedings. p. 2079.

Weiss, B.P. and Tikoo, S.M., 2014. The lunar dynamo. Science. 346(6214), 1246753.

Wieler, R., 1998. The solar noble gas record in lunar samples and meteorites. Space Science Reviews. 85, 303-314.

Wieler, R., 2002a. Noble gases in the solar system. Reviews in Mineralogy and geochemistry. 47, 21-70.

Wieler, R., 2002b. Cosmic-ray-produced noble gases in meteorites. Reviews in Mineralogy and geochemistry. 47, 125-170.

Wieler, R., 2016. Do lunar and meteoritic archives record temporal variations in the composition of solar wind noble gases and nitrogen? A reassessment in the light of Genesis data. Chemie der Erde-Geochemistry. 76, 463-480.

Wieler, R., Heber, V., 2003. Noble gas isotopes on the Moon. Space science reviews. 106, 197-210.

Wittenberg, L.J., Sarantius, J.F., Kulcinski, G.L. 1986. Lunar source of ^{3}He for commercial fusion. Fusion Technology. 10: 167-178.

9. Tables

Table 1: The range in isotope ratios for Ne and Ar (taken from Table S2). These data are only for bulk samples, except for the lunar meteorite data which is all the available data from Mészáros et al. (2018).

Rock Type	***Ratio***				
	$^{20}Ne/^{22}Ne$	**$^{20}Ne/^{22}Ne$**	**$^{21}Ne/^{22}Ne$**	**$^{38}Ar/^{36}Ar$**	**$^{40}Ar/^{36}Ar$**
database	**min - max**	**trapped**	**min - max**	**min - max**	**min - max**
Soils	1.09 - 13.7	13.3	0.03 - 0.8	0.18 – 1.30	0.09 - 469
Regolith breccias	1.25 – 13.7	12.7	0.003 - 0.833	0.18 - 0.86	0.47 - 6535
Sub-surface	11.9 - 12.8	11.9	0.03 - 0.05	0.18 - 0.19	0.74 – 2.87
Crystalline	0.62 – 13.3	12.1	0.04 - 0.92	0.17 -1.57	0.63 - 1057
Impact-melt	0.83 - 12.9	12.5	0.03 - 0.87	0.19 - 1.33	0.64 - 20509
Meteorites	0.79 - 12.9	12.4	0.03 - 1.13	0.17 - 1.51	1.11 - 10690
*literature**					
Solar wind (SW)	13.78±0.03	**-**	0.0329±0.0001	0.1828±0.0334	**-**
Cosmogenic (Cos)	0.8	**-**	0.76	1.5386	**-**
Fractionated solar wind (fSW)	11.2-12.5		0.0295	0.1886	**-**

**Taken from Heber et al., (2009) and Wieler (2002a) and references therein.*

10. Figures

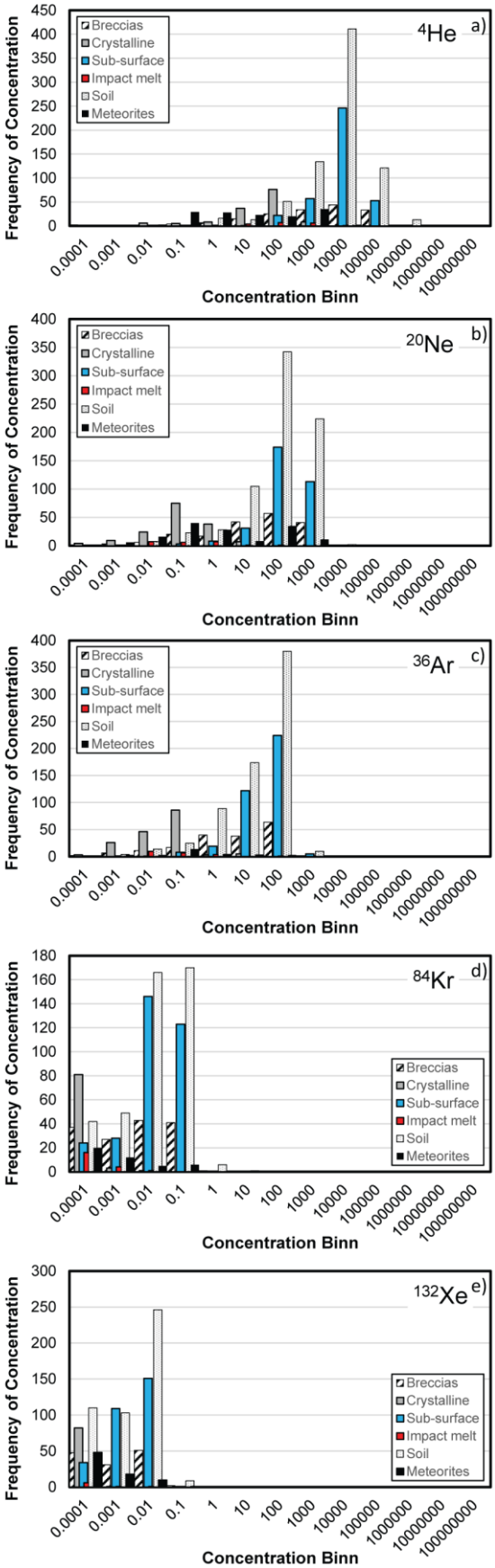
a)
^{4}He
b)
^{20}Ne
c)
^{36}Ar
d)
^{84}Kr
e)
^{132}Xe
Breccias
Crystalline
Sub-surface
Impact melt
Soil
Meteorites
Frequency of Concentration
Concentration Binn
0.0001
0.001
0.01
0.1
1
10
100
1000
10000
100000
1000000
10000000
100000000

Figure 1: Noble gas abundance data for a suite of lunar soils, regolith breccias, sub-surface, crystalline and impact-melt samples from Table S2. These data are normalised to a mass of 1 mg for a) ^{4}He, b) ^{20}Ne, c) ^{36}Ar, d) ^{84}Kr and e) ^{132}Xe concentrations (in 10^{-8} cm^{3} STP/mg). Data for lunar meteorites comes from Mészáros et al. (2018).

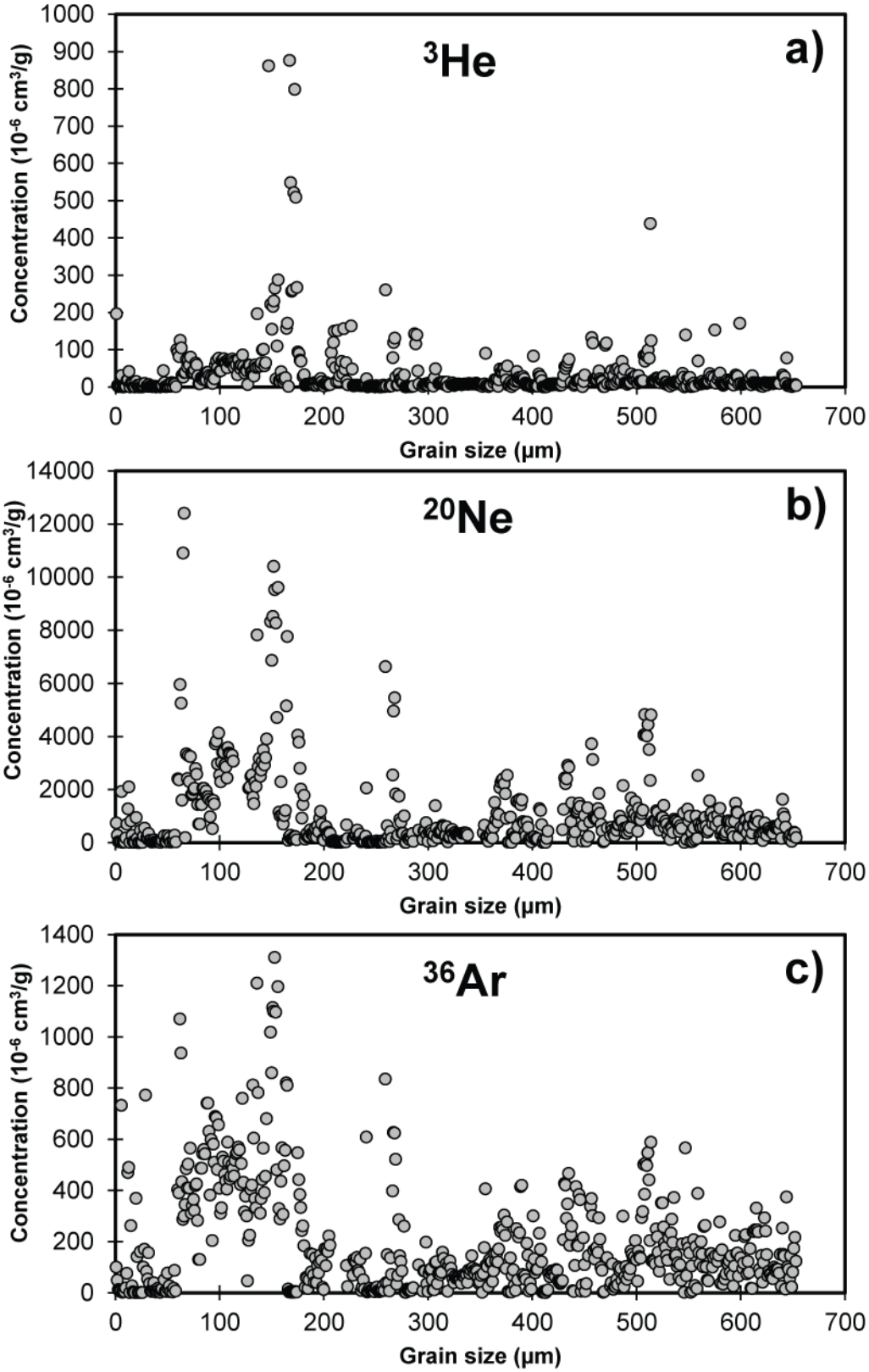

Figure 2: Noble gas concentrations for grain size separates from soils, breccia and sub-surface samples reported in Table S2. Grains size versus a) ^{3}He, b) ^{20}Ne , and c) ^{36}Ar . Note that the concentrations are in 10^{-6} cm^{3}STP/g.

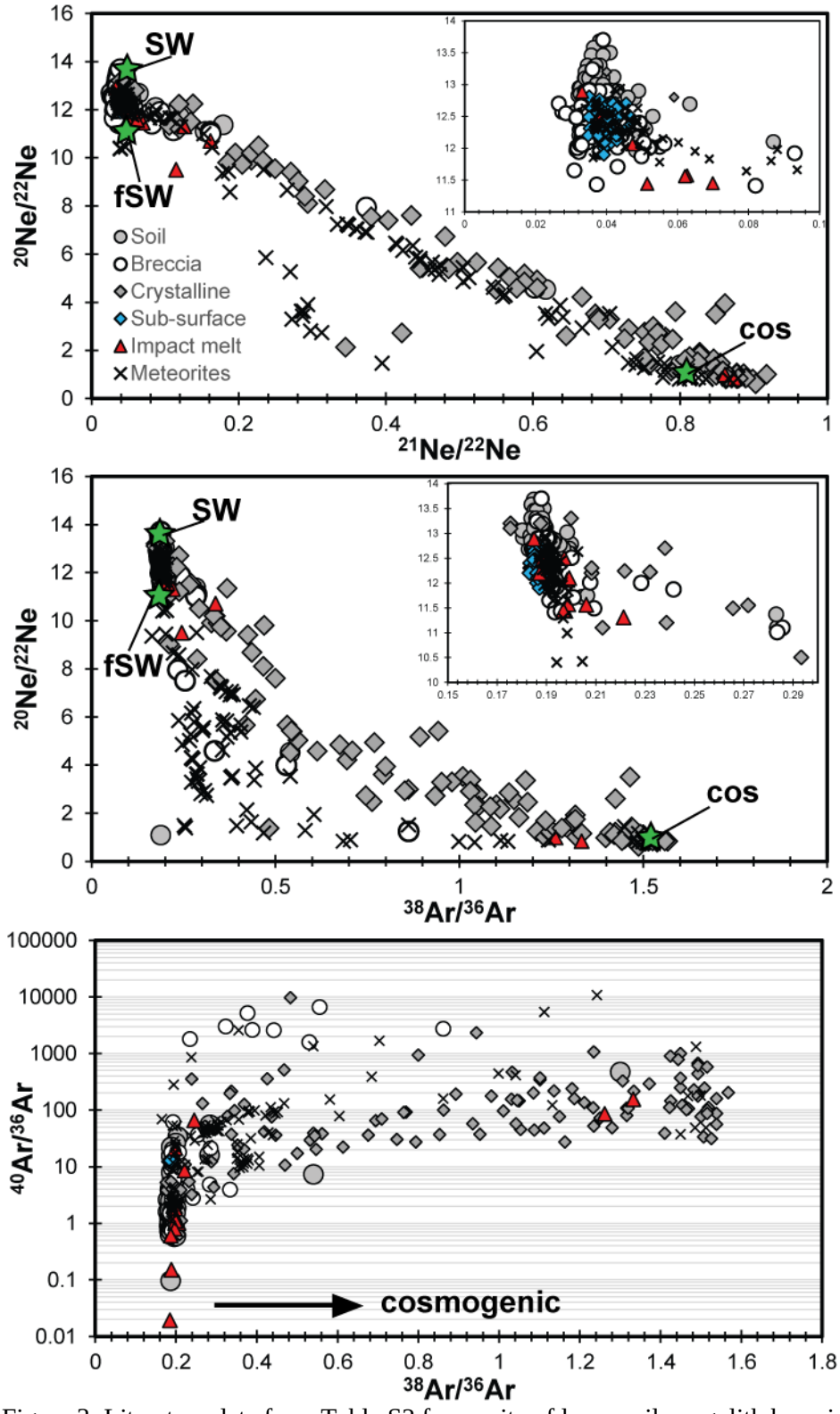

Figure 3: Literature data from Table S2 for a suite of lunar soils, regolith breccias, sub-surface, crystalline and impact-melt samples for ratios of a) $^{20}Ne/^{22}Ne$ vs. $^{21}Ne/^{22}Ne$, b) $^{20}Ne/^{22}Ne$ vs. $^{38}Ar/^{36}Ar$, and c) $^{38}Ar/^{36}Ar$ vs. $^{40}Ar/^{36}Ar$. The notation "fSW", "SW' and "cos" denote "fractionated solar wind", "solar wind" and "cosmogenic" end-members, respectively (Table 1). Inset graphs on a) and b) are close ups of the solar-dominated region. Data from lunar meteorites comes from Mészáros et al. (2018).

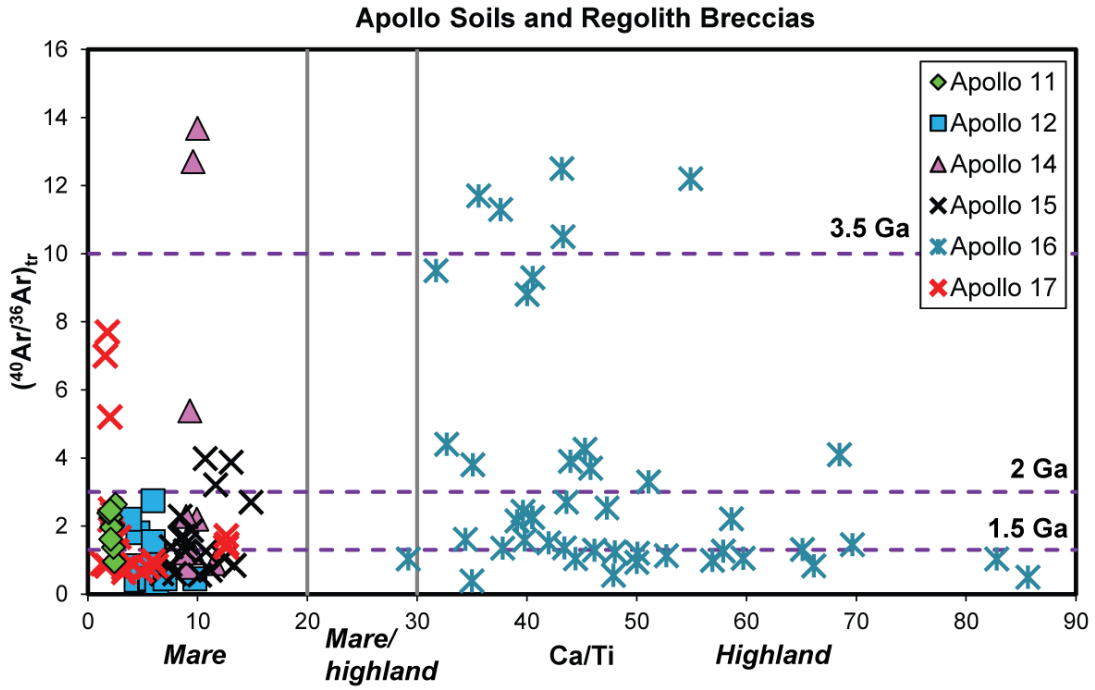

Figure 4: Ratios of Ca/Ti versus $(^{40}Ar/^{36}Ar)_{tr}$ for Apollo soils and regolith breccias (data from Table S2). The Ca/Ti ratio is used as an indicator of provenance (e.g., highland or mare, Lorenzetti et al. 2005) as the Ca concentration is higher and the Ti concentration is lower in highland rocks compared to mare-dominated material. The Ca/Ti ratios <20 are defined as mare material, highland material are defined at Ca/Ti ratios >30, and Ca/Ti ratios between 20 and 30 represents mixtures of the two provenances (e.g., a mare-highland boundary). The $(^{40}Ar/^{36}Ar)_{tr}$ derived trapped ages are provided here are an estimate and we note that there could be up to 50% errors on these estimates.

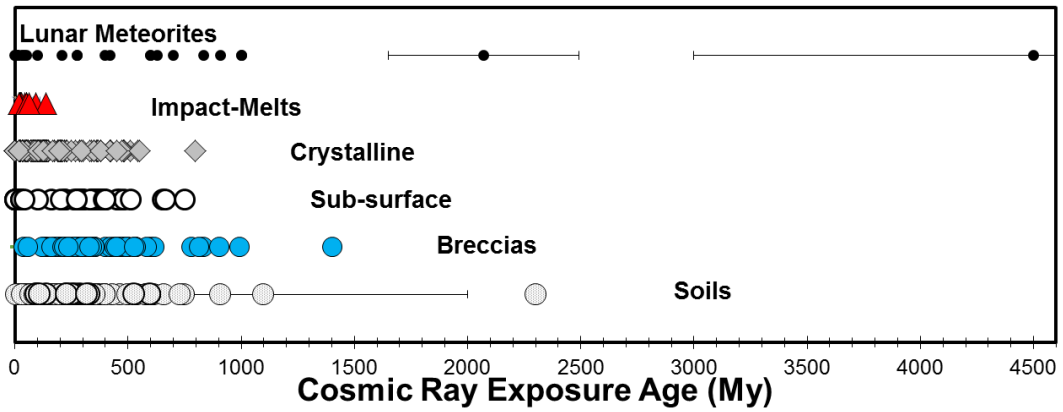

Figure 5: Exposure ages (in million years, My) of lunar soils, regolith breccias, crystalline, impact-melt and meteorite samples. Data are from Table S2 and S3.

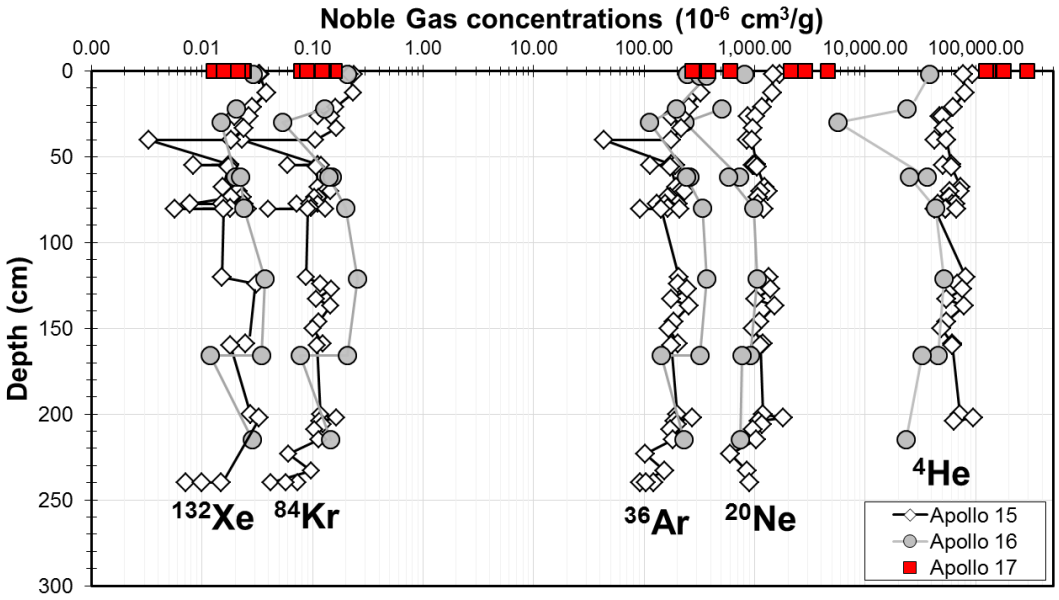

Figure 6: Noble gas concentration (^{4}He, ^{20}Ne, ^{36}Ar, ^{84}Kr and ^{132}Xe) variations with depth for Apollo 15, 16 and 17 sub-surface samples. The data are bulk samples from Table S2 (no grain size separates are included). The data are originally from Bogard and Nyquist, 1973; Hubner et al., 1973 and Jordan and Heymann, 1975.

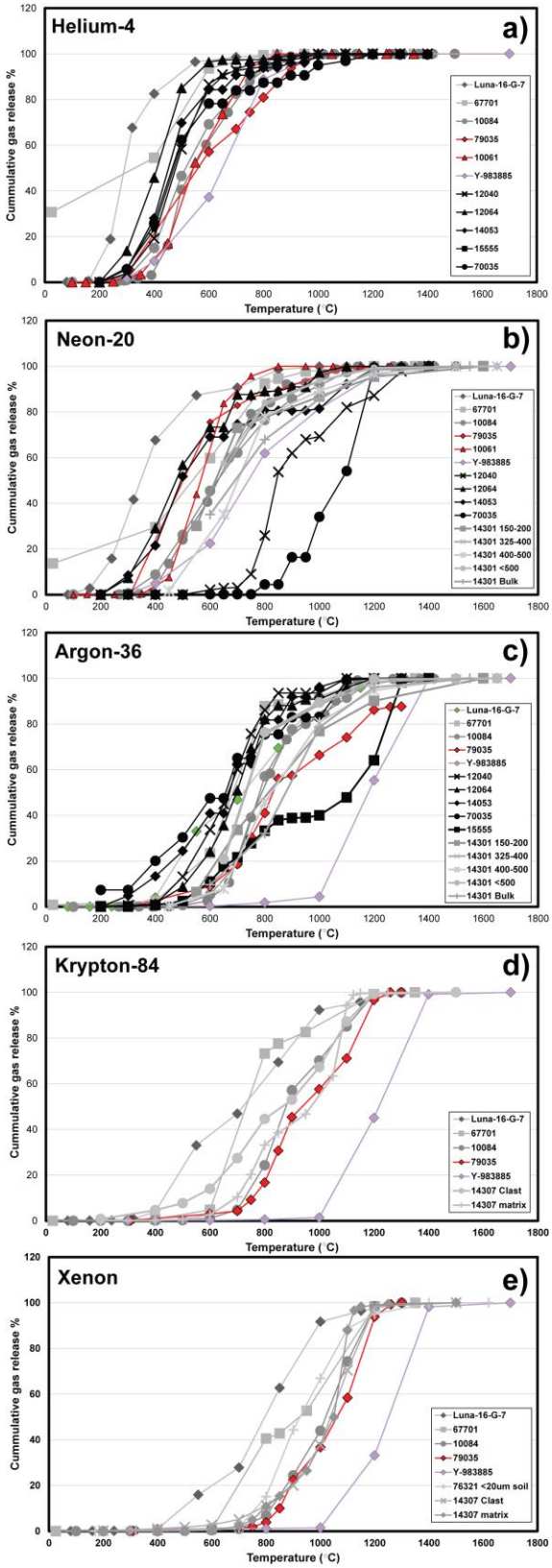

Figure 7: Cumulative temperature release profiles for a) ^{4}He, b) ^{20}Ne, c) ^{36}Ar, d) ^{84}Kr and e) ^{132}Xe in a series of lunar rock types including soil, regolith breccia, crystalline and meteorite samples. Data is compiled is Table S2 and sourced from Hohenberg et al., 1970; Pepin et al., 1970; Kaiser, 1971;

Bogard et al., 1974; Bernatowicz et al., 1977; Frick et al., 1988; Mahajan, 2015; and Mortimer et al., 2015.

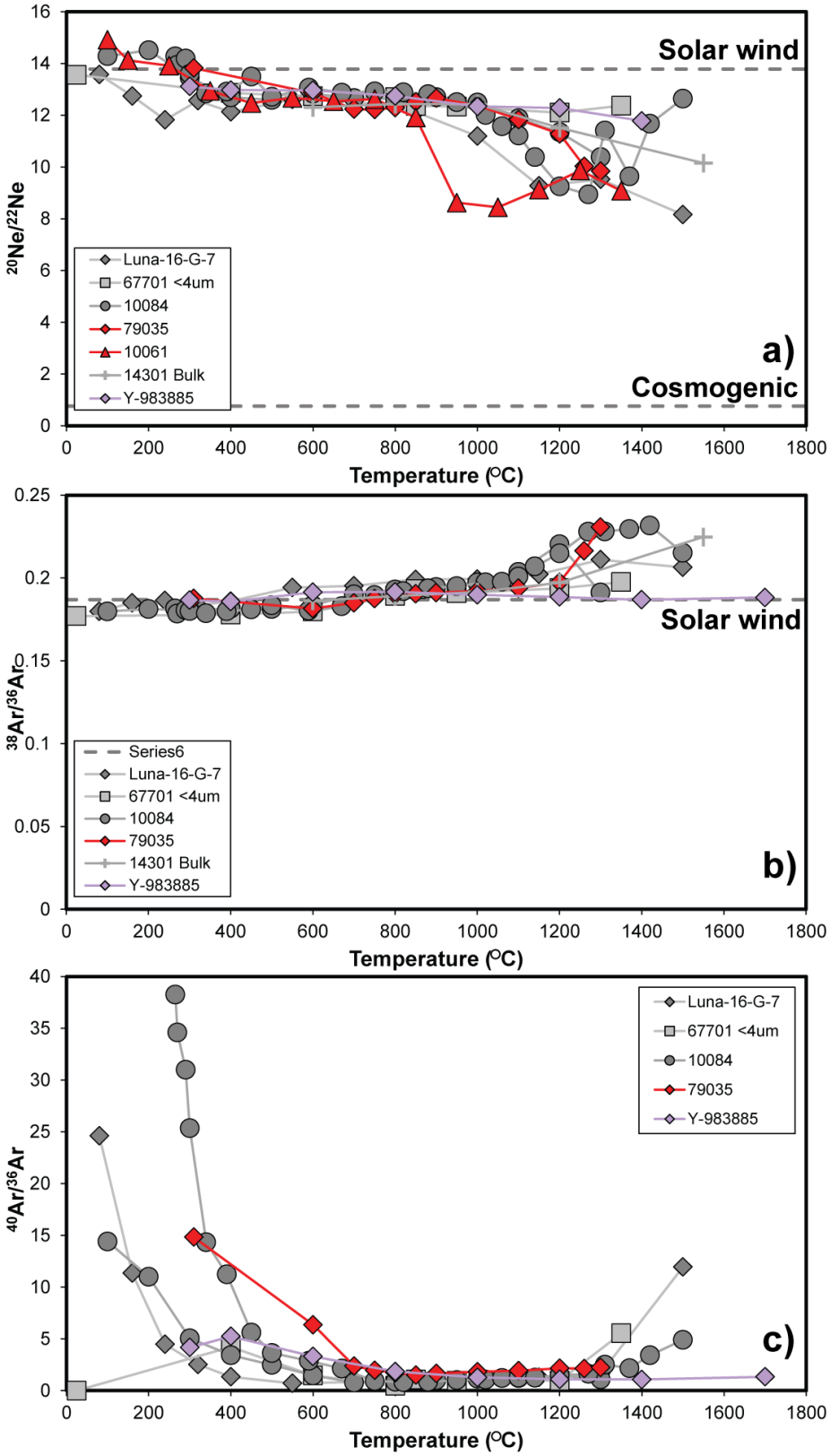

Figure 8: Temperature release profiles for noble gas ratios of a) $^{20}Ne/^{22}Ne$, b) $^{38}Ar/^{36}Ar$ and c) $^{40}Ar/^{36}Ar$ for a series of lunar rock types including soil, regolith breccia, crystalline and meteorite samples from Table S2 (Hohenberg et al., 1970; Pepin et al., 1970; Kaiser, 1972; Bogard et al., 1974; Bernatowicz et al., 1977; Frick et al., 1988; and Mahajan, 2015).